

NUREG/CR-0448

HEDL-TME-78-74

DYNAMIC ANALYSIS TO ESTABLISH NORMAL SHOCK AND VIBRATION OF RADIOACTIVE MATERIAL SHIPPING PACKAGES

Quarterly Progress Report
April 1 — June 30, 1978

S R. Fields

S. J. Mech

Hanford Engineering Development Laboratory

120555003927 2 RTAN
US NRC
SECY PUBLIC DOCUMENT ROOM
BRANCH CHIEF
HST LOBBY
WASHINGTON DC 20555

Prepared for
U. S. Nuclear Regulatory Commission

790124 0094

NOTICE

This report was prepared as an account of work sponsored by an agency of the United States Government. Neither the United States Government nor any agency thereof, or any of their employees, makes any warranty, expressed or implied, or assumes any legal liability or responsibility for any third party's use, or the results of such use, of any information, apparatus product or process disclosed in this report, or represents that its use by such third party would not infringe privately owned rights.

Available from
National Technical Information Service
Springfield, Virginia 22161
Price: Printed Copy \$4.50 ; Microfiche \$3.00

The price of this document for requesters outside of the North American Continent can be obtained from the National Technical Information Service.

DYNAMIC ANALYSIS TO ESTABLISH NORMAL SHOCK AND VIBRATION OF RADIOACTIVE MATERIAL SHIPPING PACKAGES

**Quarterly Progress Report
April 1 — June 30, 1978**

S. R. Fields
S. J. Mech

Manuscript Completed: July 1978
Date Published: December 1978

Hanford Engineering Development Laboratory
P. O. Box 1970
Richland, WA 99352

Division of Safeguards, Fuel Cycle, and Environmental Research
Office of Nuclear Regulatory Research
U. S. Nuclear Regulatory Commission
Under Contract No. NRC-60-78-354

Dynamic Analysis to Establish Normal
Shock and Vibration
of Radioactive
Material Shipping Packages

Quarterly Progress Report
April 1 - June 30, 1978

S. R. Fields
S. J. Mech

ABSTRACT

This report presents work performed at the Hanford Engineering Development Laboratory operated by Westinghouse Hanford Company, a subsidiary of Westinghouse Electric Corporation, for the Nuclear Regulatory Commission, under Department of Energy Contract No. EY-76-C-14-2170. It describes technical progress made during the reporting period by Westinghouse Hanford Company and supporting contractors.

CONTENTS

	<u>Page</u>
ABSTRACT	iii
FIGURES	vii
SUMMARY	ix
INTRODUCTION	1
PROGRESS TO DATE	2
1. Develop Dynamic Model	2
2. Data Collection and Reduction	12
3. Validate Model	23
4. Collect Parameter Data	25
5. Parametric and Sensitivity Analysis	25
6. Interim Report	25
7. Final Report	25
REFERENCES	26

FIGURES

		<u>Page</u>
1	Work Plan -- Dynamic Analysis of Radioactive Material Shipping Packages	3
2	Spring-Mass-Dashpot Model of the Cask-Rail Car Coupler Subsystem	4
3	Comparison of Orientation of Cask-Rail Car System After Impact with Initial State	13
4a	Acceleration Wave Shape and Corresponding Frequency Spectrum Obtained by Fast Fourier Transform (Horizontal Center Acceleration)	15
4b	Acceleration Wave Shape and Corresponding Frequency Spectrum Obtained by Fast Fourier Transform (Vertical, Struck End Acceleration)	16
4c	Acceleration Wave Shape and Corresponding Frequency Spectrum Obtained by Fast Fourier Transform (Vertical, Far End Acceleration)	17
5a	Filtering of Acceleration Data Employing Inverse FFT (Power Spectra and Time Domain Image)	18
5b	Filtering of Acceleration Data Employing Inverse FFT (Time Domain Images)	19
6a	Hanning Window Effect on Power Spectra When Applied to Time Domain Data (Horizontal, Center Acceleration with Hanning Window)	21
6b	Hanning Window Effect on Power Spectra When Applied to Time Domain Data (Vertical, Struck End Acceleration with Hanning Window)	22
7	Pseudo-Isometric Illustrations of Car Acceleration and Displacement as It Varies with Time	24

DYNAMIC ANALYSIS TO ESTABLISH NORMAL
SHOCK AND VIBRATION OF RADIOACTIVE
MATERIAL SHIPPING PACKAGES

Quarterly Progress Report
April 1, 1978 - June 30, 1978

SUMMARY

DEVELOP DYNAMIC MODEL

A calculation sequence was developed to simulate the behavior of the coupler subsystem for the cask-rail car and the lead car it impacts during humping operations. This coupler submodel was tested successfully, but additional development and better input data are required. The results must be compared to the actual performance of a coupler before the submodel can be considered an accurate simulation.

DATA COLLECTION AND REDUCTION

To test the proposed data reduction and model verification techniques, data were synthesized using the current cask-rail car simulation model. Acceleration data from the model for three selected locations were operated on by Fast Fourier Transforms (FFT) to produce the frequency domain equivalent to the original time domain data generated. The results of this process are equivalent to those derived from a spectrum analyzer -- power spectral density. The application of various filtering and other techniques for analyzing such data were demonstrated.

VALIDATE MODEL

A technique is described that will be used initially to reduce experimental data, obtained from the rail car humping tests at the Savannah River Laboratories, to a form suitable for use in validation of the cask-rail car simulation model.

INTRODUCTION

This study was initiated in October, 1977 as stated earlier in the previous quarterly progress report. The objective of this study is to determine the extent to which the shocks and vibrations experienced by radioactive material shipping packages during normal transport conditions are influenced by, or are sensitive to, various structural parameters of the transport system (i.e., package, package supports, and vehicle). The purpose of this effort is to identify those parameters which significantly affect the normal shock and vibration environments so as to provide the basis for determining the forces transmitted to radioactive material packages. Determination of these forces will provide the input data necessary for a broad range of package-tiedown structural assessments.

This is the third quarterly report on this work. A work plan, consisting of seven tasks, was presented in the first and second quarterly reports [NUREG/CR-0071 (HEDL-TME 78-19) and NUREG/CR-061 (HEDL-TME 78-41), respectively]. Progress on these tasks during this reporting period will now be discussed.

PROGRESS TO DATE

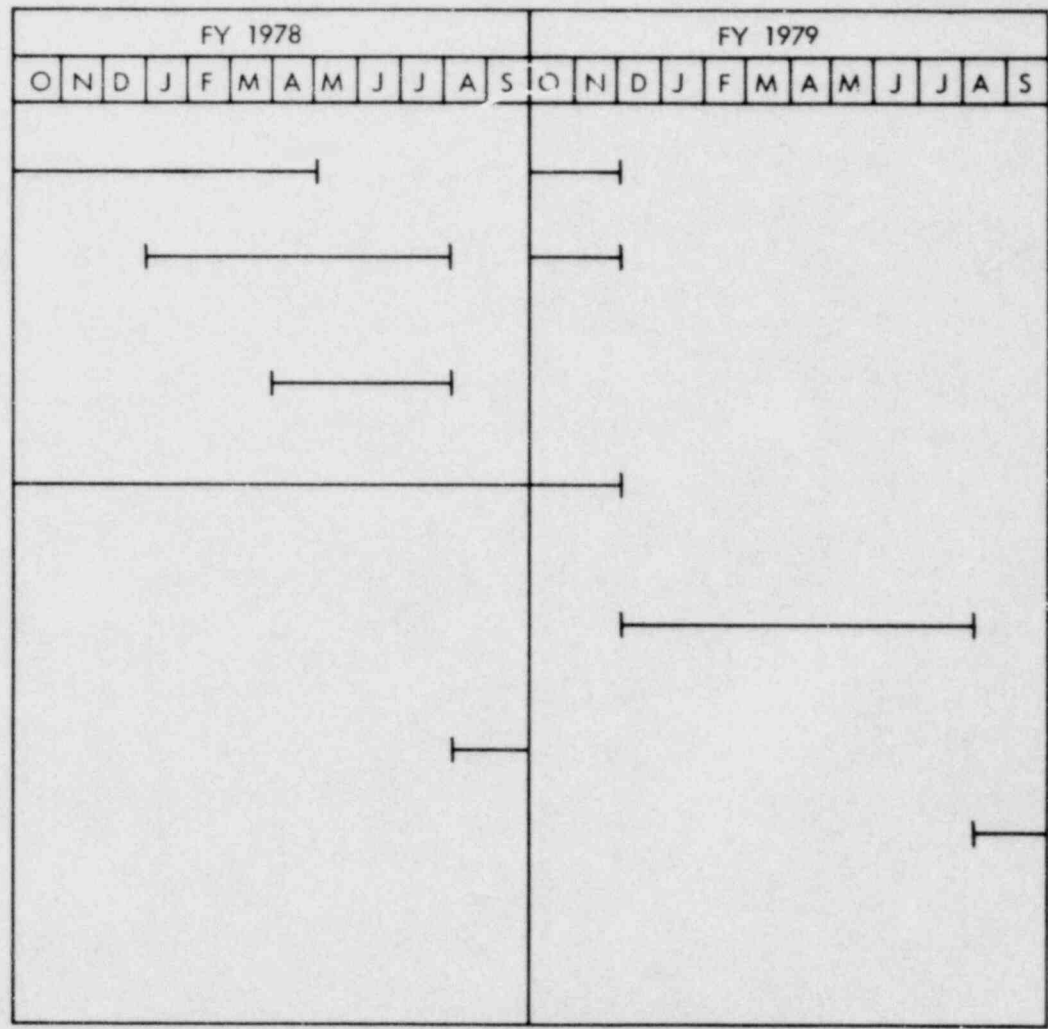
The work plan for this study, presented as Figure 1, shows the various tasks and their relation to one another. The progress on each of these tasks during this reporting period will now be discussed.

1. Develop Dynamic Model

A calculation sequence has been developed to simulate the behavior of the coupler subsystem for the cask-rail car and the lead car in the group it impacts during humping operations. This coupler submodel determines the displacements of the springs and dampers (dashpots) during normal operating conditions, and the displacements and other conditions when one or more of these components bottom out at their limits of travel. The submodel has been tested successfully, but some additional developmental effort and better input data are required.

The coupler subsystem is represented by two Maxwell bodies in series, one attached to the spring representing the cask-rail car and the other attached to the spring representing the lead car in the struck group (see Figure 2). A Maxwell body is one which exhibits linear viscoelastic behavior and is represented by a spring and dashpot in series. A mathematical model of this coupler subsystem (coupler submodel) has been developed using the energy method. The equations obtained have been verified using an alternate approach.

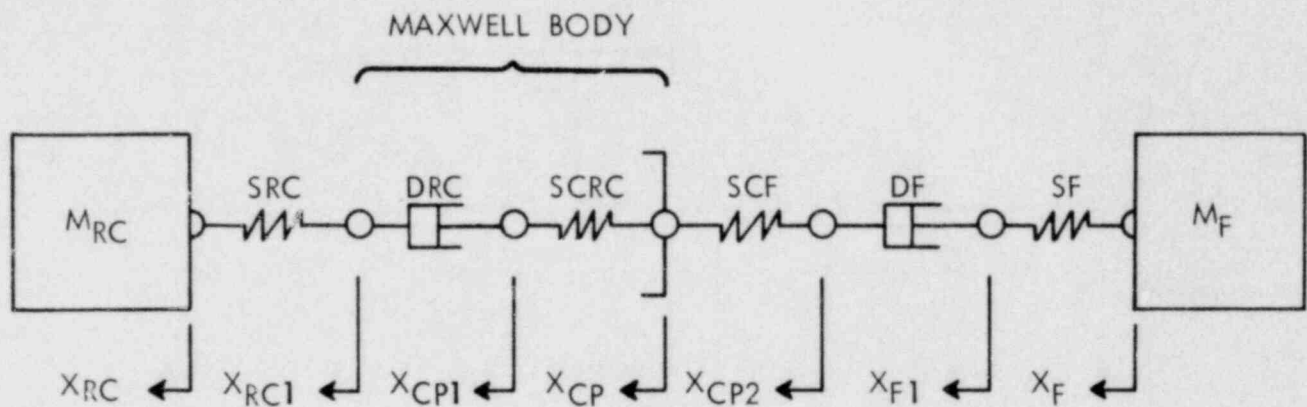
The energy method was used earlier to derive the equations of motion for the spring-mass-dashpot model of the complete cask-rail car system (see the first quarterly report NUREG/CR-0071 [HEDL-TME 78-19]). These equations of motion were derived from an energy balance (expressed in generalized coordinates) on the system. This energy balance, sometimes referred to as the law of virtual work, states that the work done on the system by the external forces (virtual work) during a virtual distortion (a small change in one of the generalized coordinates) must equal the change in internal strain energy. The work done by external forces includes the work done by external loads, by inertia forces, and by damping or dissipation



3

HEDL 7803-106.1

FIGURE 1. Work Plan -- Dynamic Analysis of Radioactive Material Shipping Packages.



HEDL 7811-042.1

- | | |
|------|---|
| SRC | Spring representing the cask-rail car |
| DRC | Damper in the cask-rail car coupler subsystem |
| SCRC | Spring in the cask-rail car coupler subsystem |
| SCF | Spring in the struck car coupler subsystem |
| DF | Damper in the struck car coupler subsystem |
| SF | Spring representing the struck car |

FIGURE 2. Spring-Mass-Dashpot Model of the Cask-Rail Car Coupler Subsystem.

forces. It can be shown that the changes in the energy terms with respect to a change in a generalized coordinate may be expressed as partial derivatives, and that the energy balance on the system may be expressed as

$$\frac{d}{dt} \left(\frac{\partial K}{\partial \dot{q}_i} \right) - \frac{\partial K}{\partial q_i} + \frac{\partial U}{\partial q_i} - \frac{\partial W_c}{\partial q_i} = \frac{\partial W_e}{\partial q_i}$$

where

- t = time,
- q_i = a generalized coordinate,
- \dot{q}_i = time rate of change of q_i ,
- K = kinetic energy,
- U = strain energy or potential energy,
- W_c = work done by damping forces,
- W_e = work done by external loads.

This equation is one form of Lagrange's equation. When appropriate expressions are written for K, U, W_c and W_e , all in terms of the generalized coordinates q_1, q_2, \dots, q_n , differentiated as indicated, and substituted into the above expression, equations of motion are obtained. There will be one equation of motion for each of the n coordinates or degrees of freedom. In all cases considered, $\frac{\partial K}{\partial q_i}$ is zero, since kinetic energy is a function of velocity rather than displacement.

The energy method was applied to the coupler subsystem of Figure 2 as follows:

- (1) The junction points X_{RC} and X_F have masses M_{RC} and M_F , respectively. All other junction points are treated as zero mass points.

(2) Junction point X_{RC} :

Generalized coordinate:

$$q_j = X_{RC}$$

Kinetic energy:

$$K = 1/2 M_{RC} \dot{X}_{RC}^2, \quad (1)$$

$$\therefore \frac{\partial K}{\partial \dot{X}_{RC}} = M_{RC} \dot{X}_{RC}, \quad (2)$$

$$\frac{d}{dt} \left(\frac{\partial K}{\partial \dot{X}_{RC}} \right) = M_{RC} \ddot{X}_{RC}, \quad (3)$$

$$\text{and } \frac{\partial K}{\partial X_{RC}} = 0. \quad (4)$$

Potential or strain energy:

$$U = \frac{k_{SRC}}{2} (X_{RC} - X_{RC1})^2 \quad (5)$$

$$\therefore \frac{\partial U}{\partial X_{RC}} = k_{SRC} (X_{RC} - X_{RC1}) \quad (6)$$

Damping forces:

$$W_c = 0 \quad (7)$$

External forces:

$$W_e = 0. \quad (8)$$

The energy balance on the mass M_{RC} may be expressed as

$$\frac{d}{dt} \left(\frac{\partial K}{\partial \dot{x}_{RC}} \right) - \frac{\partial K}{\partial x_{RC}} + \frac{\partial U}{\partial x_{RC}} - \frac{\partial W_c}{\partial x_{RC}} = \frac{\partial W_e}{\partial x_{RC}} \quad (9)$$

or, upon substitution from equations (3), (4), (6), (7) and (8), as

$$M_{RC} \ddot{x}_{RC} - 0 + k_{SRC} (x_{RC} - x_{RC1}) - 0 = 0 \quad (10)$$

or

$$M_{RC} \ddot{x}_{RC} + k_{SRC} (x_{RC} - x_{RC1}) = 0 \quad (11)$$

(3) Junction point x_{RC1} :

Generalized coordinate:

$$q_i = x_{RC1}$$

Kinetic energy: Since $M_{RC1} = 0$, all kinetic energy terms are zero.

Potential or strain energy:

$$U = \frac{k_{SRC}}{2} (x_{RC} - x_{RC1})^2 \quad (12)$$

$$\therefore \frac{\partial U}{\partial x_{RC1}} = -k_{SRC} (x_{RC} - x_{RC1}) \quad (13)$$

Damping forces:

$$W_c = -C_{DRC} (\dot{x}_{RC1} - \dot{x}_{CP1}) (x_{RC1} - x_{CP1}) \quad (14)$$

$$\therefore \frac{\partial W_c}{\partial x_{RC1}} = -C_{DRC} (\dot{x}_{RC1} - \dot{x}_{CP1}) \quad (15)$$

External forces:

$$\dot{W}_e = 0 \quad (16)$$

The energy balance on the zero mass junction point represented by the generalized coordinate x_{RC1} may be expressed as

$$\frac{d}{dt} \left(\frac{\partial K}{\partial \dot{x}_{RC1}} \right) - \frac{\partial K}{\partial x_{RC1}} + \frac{\partial U}{\partial x_{RC1}} - \frac{\partial W_c}{\partial x_{RC1}} = \frac{\partial W_e}{\partial x_{RC1}} \quad (17)$$

or, upon substitution of equations (13), (15) and (16), as

$$0 - 0 - k_{SCR}(x_{RC} - x_{RC1}) - C_{DRC}(\dot{x}_{RC1} - \dot{x}_{CP1}) = 0 \quad (18)$$

or

$$k_{SRC}(x_{RC} - x_{RC1}) = C_{DRC}(\dot{x}_{RC1} - \dot{x}_{CP1}). \quad (19)$$

- (4) Applying the above procedure to the remaining junction points, the following additional equations are obtained:

Generalized Coordinate q_i	Equation
x_{CP1}	$k_{SCRC}(x_{CP1} - x_{CP}) = C_{DRC}(\dot{x}_{RC1} - \dot{x}_{CP1}) \quad (20)$
x_{CP}	$k_{SCRC}(x_{CP} - x_{CP1}) = k_{SCF}(x_{CP2} - x_{CP}) \quad (21)$
x_{CP2}	$k_{SCF}(x_{CP2} - x_{CP}) = C_{DF}(\dot{x}_{F1} - \dot{x}_{CP2}) \quad (22)$
x_{F1}	$C_{DF}(\dot{x}_{F1} - \dot{x}_{CP2}) = k_{SF}(x_F - x_{F1}) \quad (23)$
x_F	$M_F \ddot{x}_F + k_{SF}(x_{F1} - x_F) = 0 \quad (24)$

The equations of motion for the masses M_{RC} and M_F are equations (11) and (24), respectively. In the actual cask-rail car model, these equations contain many additional terms representing the potential energy and dissipation energy due to the relationship of the masses to other components in the system. These additional terms include the vertical and rotational contributions as well as the axial contributions. Equations (11) and (24) were simplified here for demonstration purposes.

In the complete cask-rail car model, the displacements of the mass points are obtained by integration of the respective equations of motion. The displacements of the zero mass points (coupler subsystem junction points) are determined by an iterative procedure using equations (19) through (23).

These equations are rewritten to yield the displacements:

$$X_{RC1} = (k_{DRC} X_{CP1P} + k_{SRC} X_{RC}) / (k_{DRC} + k_{SRC}) \quad (25)$$

$$X_{CP1} = (k_{SCRC} X_{CPP} + k_{DRC} X_{RC1P}) / (k_{SCRC} + k_{DRC}) \quad (26)$$

$$X_{CP} = (k_{SCF} X_{CP2P} + k_{SCRC} X_{CP1P}) / (k_{SCF} + k_{SCRC}) \quad (27)$$

$$X_{CP2} = (k_{DF} X_{F1P} + k_{SCF} X_{CPP}) / (k_{DF} + k_{SCF}) \quad (28)$$

$$X_{F1} = (k_{SF} X_F + k_{DF} X_{CP2P}) / (k_{SF} + k_{DF}) \quad (29)$$

where X_{RC1P} , X_{CP1P} , X_{CPP} , X_{CP2P} and X_{F1P} are the values of X_{RC1} , X_{CP1} , X_{CP} , X_{CP2} and X_{F1} obtained from the previous calculation in the iterative procedure. The iterative procedure is entered at each time step and convergence criteria must be satisfied before time can be advanced and integrations

performed. The spring constants k_{DRC} and k_{DF} are pseudo spring constants for the dashpots. These pseudo spring constants are defined as

$$k_{DRC} = \frac{C_{DRC}}{D_{TRC}} \quad (30)$$

and

$$k_{DF} = \frac{C_{DF}}{D_{TF}} \quad (31)$$

where C_{DRC} and C_{DF} are the damping coefficients of dashpots DRC and DF, respectively, and D_{TRC} and D_{TF} are the piston travel times.

The piston travel times are determined using mode-controlled integration. A mode-controlled integrator in ACSL (Advanced Continuous Simulation Language) is expressed as

$$Y = \text{MODINT} (YD, IC, L1, L2)$$

where

YD = the derivative variable or expression,

IC = the initial condition,

L1 and L2 = logical variables or expressions of arbitrary complexity denoting the mode.

A mode-controlled integrator allows operation in RESET and HOLD modes as well as in normal OPERATE. The mode of the integrator is determined by the two logical variables L1 and L2. The truth table is

L1	L2	MODE
T	F	Reset
F	F	Operate
T	T	Operate
F	T	Hold

where T = .TRUE. and F = .FALSE.

The piston travel times are determined using the equations

$$DTRC = \text{MODINT}(1., 0., \text{NOT.NORMDR.OR.VXURCD.EQ.0.}, \text{FALSE.}) + \text{EPST} \quad (32)$$

$$\text{and } DTF = \text{MODINT}(1., 0., \text{NOT.NORMDF.OR.VXUFD.EQ.0.}, \text{FALSE.}) + \text{EPST} \quad (33)$$

with

$$YD = 1.$$

$$IC = 0.$$

$$L1 = \text{NOT.NORMDR.OR.VXURCD.EQ.0.} \quad (\text{for equation [32]})$$

$$L1 = \text{NOT.NORMDF.OR.VXUFD.EQ.0.} \quad (\text{for equation [33]})$$

$$L2 = \text{FALSE.}$$

If L1 is true, the integrator is in the RESET mode and DTRC (or DTF) is reset to the initial condition 0. If L1 is false, the integrator is in the OPERATE mode and

$$DTRC = \left(\int dt + IC \right) + \text{EPST}$$

or

$$DTF = \left(\int dt + IC \right) + \text{EPST.}$$

EPST is a small number which prevents division by zero in equations (30) and (31), and t is time. NORMDR and NORMDF are logical variables that are true

when the respective piston has not bottomed out either at full travel or at zero travel. VXURCD and VXUFD are the time derivatives of the travel of the respective pistons, i.e.,

$$VXURCD = \dot{X}_{RC1} - \dot{X}_{CP1}$$

and

$$VXUFD = \dot{X}_{CP2} - \dot{X}_{F1}$$

When these terms are zero, the pistons have either paused or changed direction and the travel time must be reset to zero.

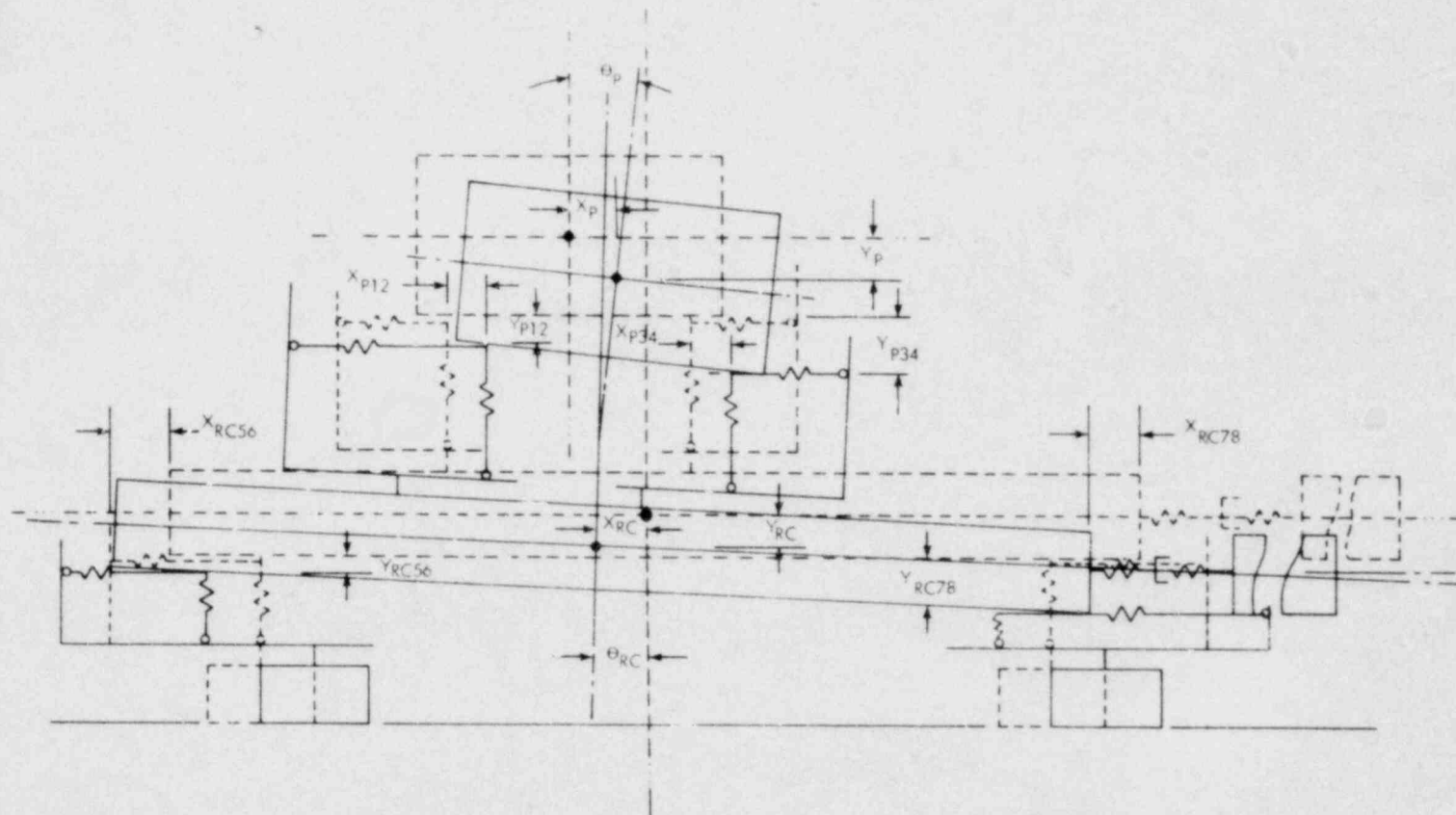
If any of the elements in the coupler submodel (Figure 2) bottom out, the respective spring constant follows a load-deflection curve or resistance function which represents "damage" or permanent deformation. This will be represented as a hysteresis-type variation of load and deflection.

2. Data Collection and Reduction

To exercise the proposed data reduction and model verification techniques, data was synthesized employing an analytical model similar to that described previously.⁽¹⁾ Specifically, an analytical model with arbitrary spring constants, damping factors, mass and dimensions was created. This model, shown in Figure 3, produced instantaneous acceleration, velocity and displacement of three locations at 0.01-second intervals for a total interval of 2 seconds.

The parameters employed in this exercise were:

- XRC - horizontal displacement at center of the rail car
- YRC56 - vertical displacement at rear of the car above support
(rear truck)
- YRC78 - vertical displacement at front of the car above support
(front truck)



HEDL 7803-106.5

FIGURE 3. Comparison of Orientation of Cask-Rail Car System After Impact with Initial State.

- DXRC - derivative of XRC, or velocity
- DYRC56 - derivative of YRC56, or velocity
- D2XRC - second derivative of XRC, or acceleration
- D2YR56 - second derivative of YRC56, or acceleration
- D2YR78 - second derivative of YRC78, or acceleration.

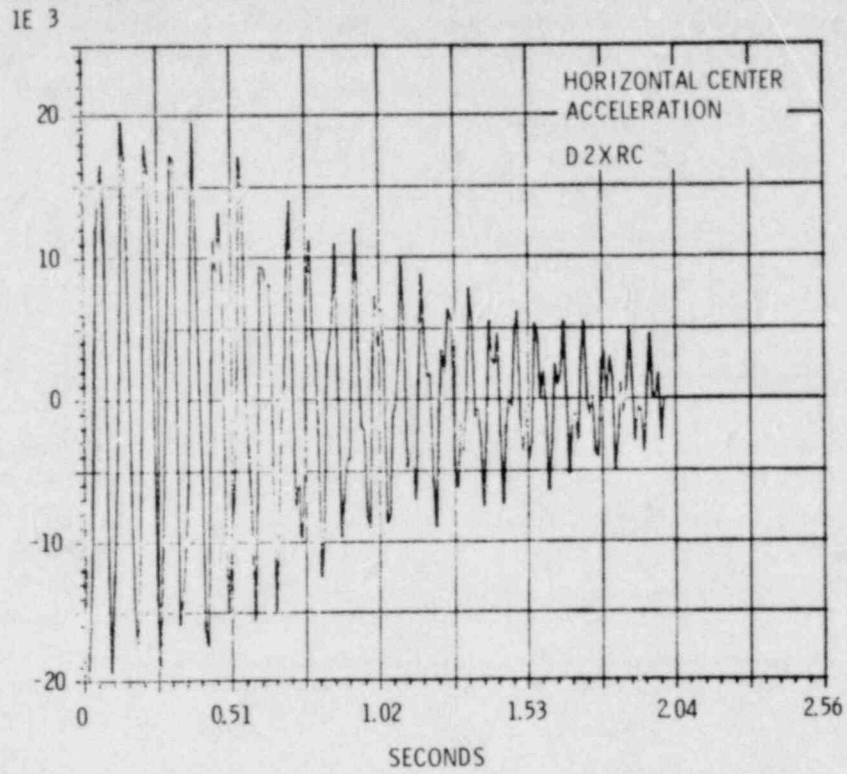
Impact is assumed to be at the "front-end" of the car.

Data obtained experimentally will generally be acceleration, but by employing the proper boundary conditions to establish the constants of integration, both the velocity and displacement data can be derived. Because of this, the displacement, velocity and acceleration data derived from the model are assumed equivalent to that which will be obtained experimentally.

Initially, the acceleration data for the three positions were operated on by Fast Fourier Transforms (FFT) producing the frequency domain equivalent of original time domain data. The results of this process, shown in Figure 4, are the same as those derived from a spectrum analyzer--power spectral density.

The inverse FFT, which transforms the frequency domain data to its time domain equivalent, offers an ideal filtering ability. If the bandwidth of the information is reduced, the time domain information is altered, as shown in Figure 5.

The example given is where the vertical acceleration on the struck end (D2YR56) is limited to 75 percent and 50 percent of the total bandwidth of 50 Hz. It should be noted that as the higher frequency information is deleted, as in the 50 percent bandwidth case, the instantaneous peak acceleration value is altered. This process, if improperly used, could misrepresent



MAGNITUDE OF FFT

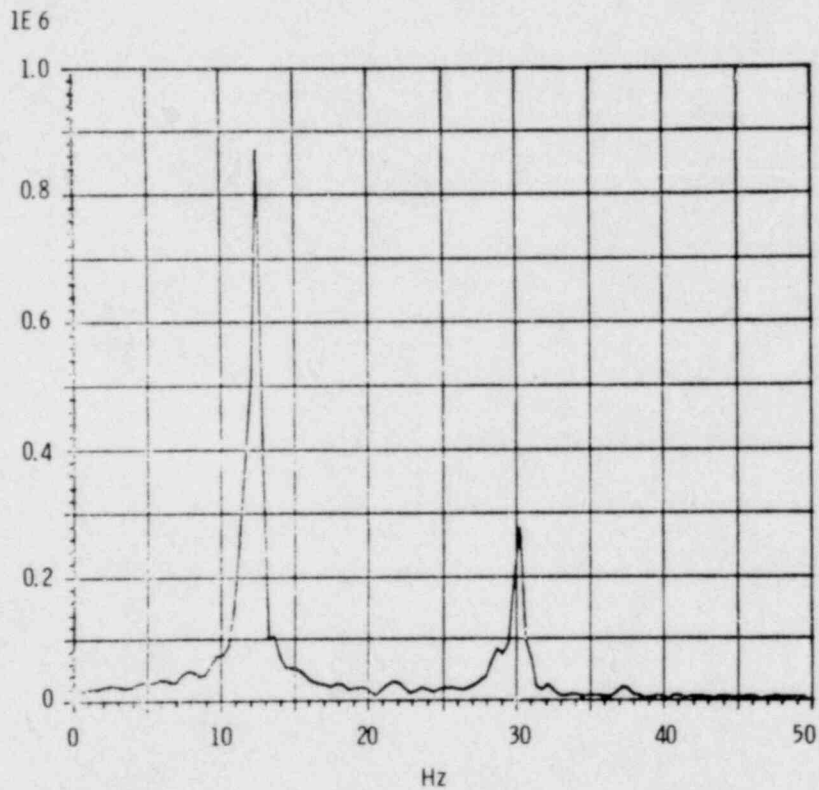


FIGURE 4a. Acceleration Wave Shape and Corresponding Frequency Spectrum Obtained by Fast Fourier Transform.

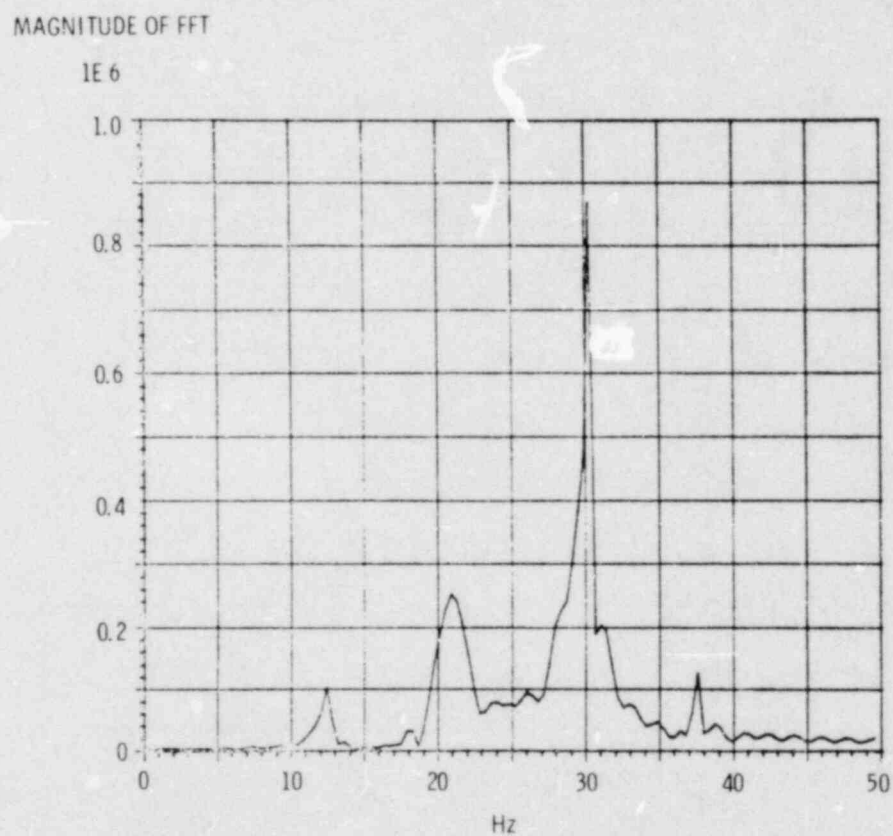
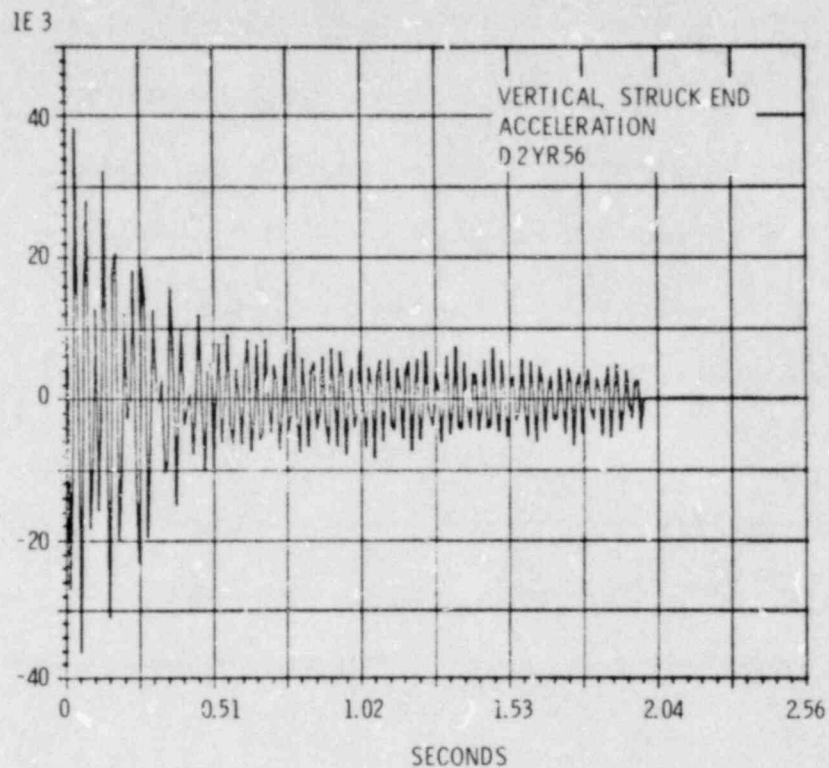
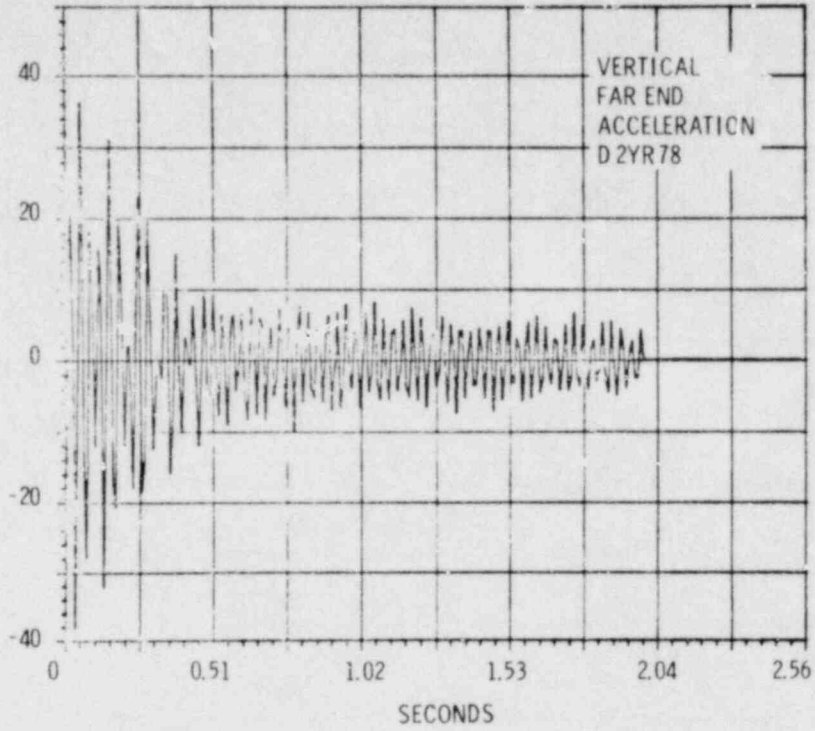


FIGURE 4b. Acceleration Wave Shape and Corresponding Frequency Spectrum Obtained by Fast Fourier Transform.

1 E 3



MAGNITUDE OF FFT (X19)

1E 6

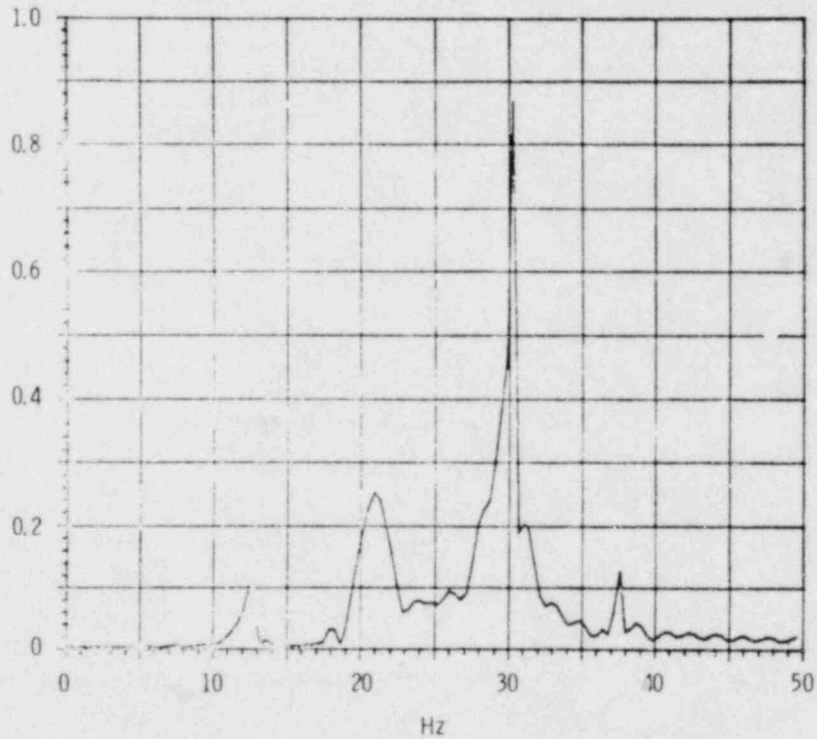


FIGURE 4c. Acceleration Wave Shape and Corresponding Frequency Spectrum Obtained by Fast Fourier Transform.

MAGNITUDE OF FFT OF D2\ .56

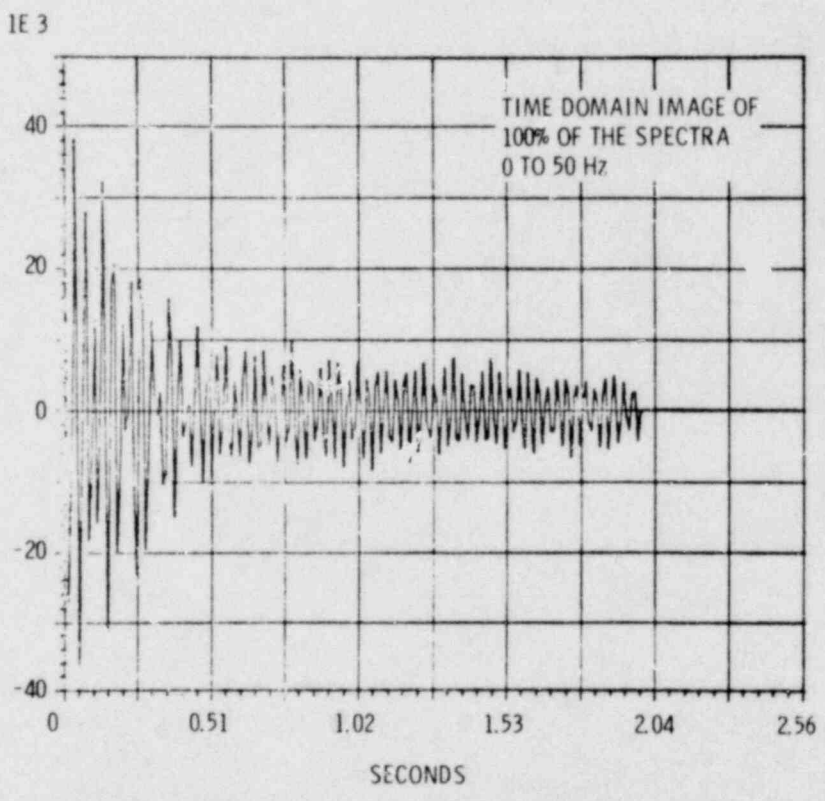
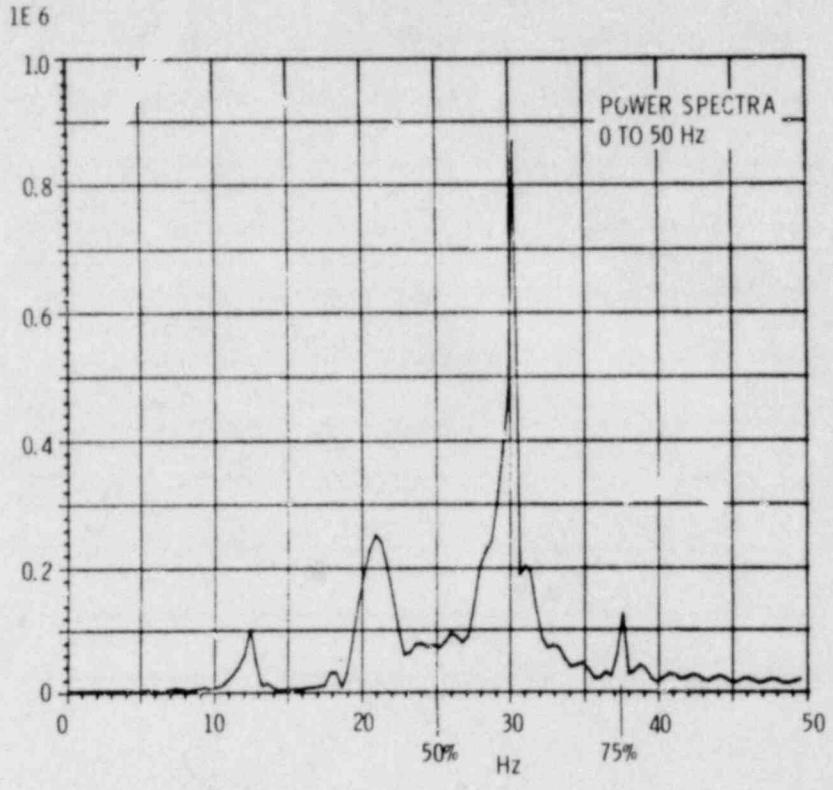
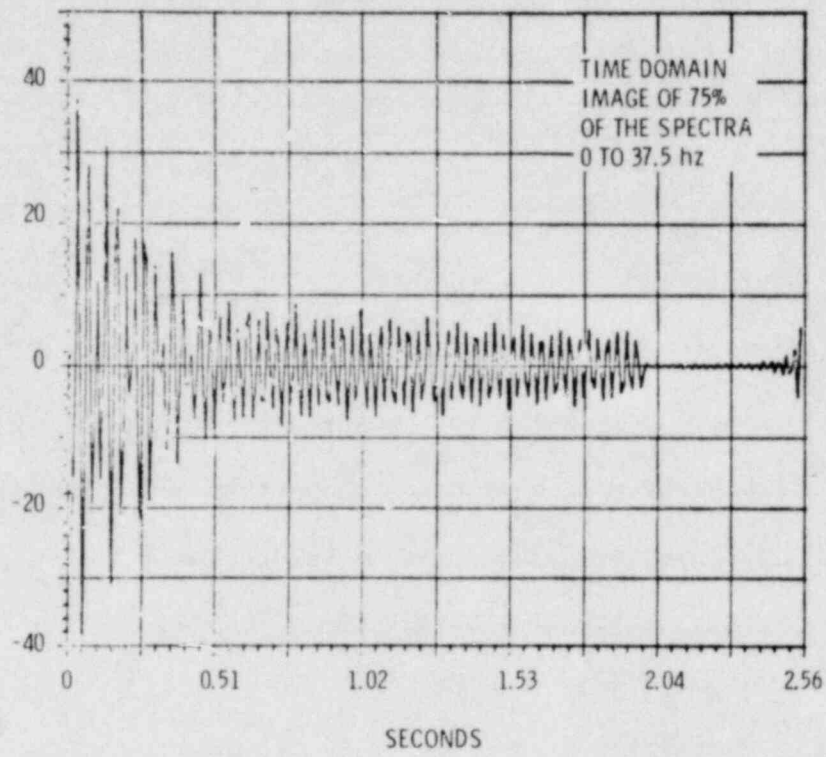


FIGURE 5a. Filtering of Acceleration Data Employing Inverse FFT.

1E 3



1E 3

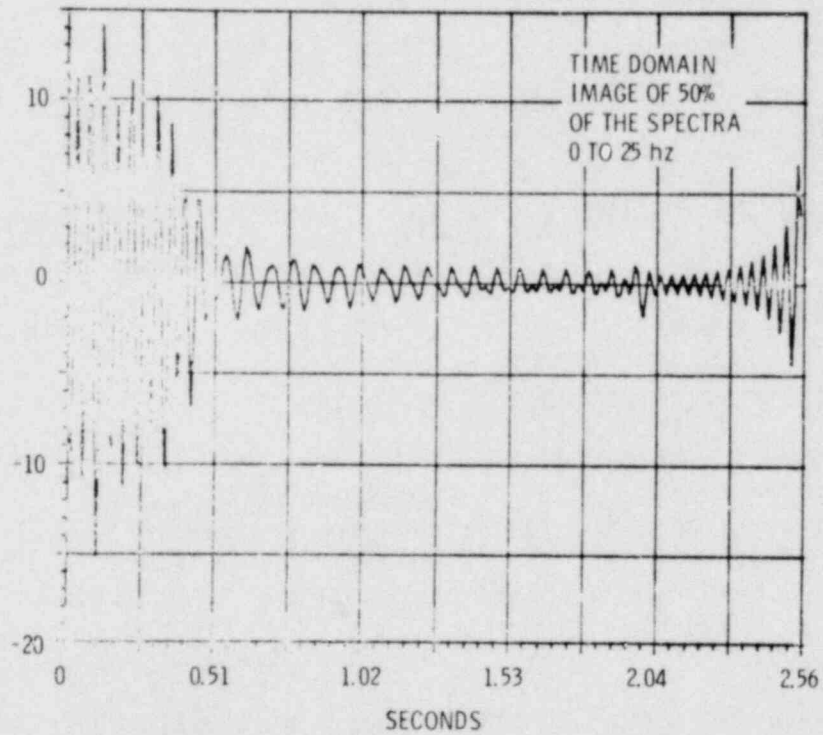


FIGURE 5b. Filtering of Acceleration Data Employing Inverse FFT.

the instantaneous peak forces in a system. Similarly, if one were to attempt to find similarities between filtered time domain waveforms, the nature of the filtering would have to be comparable.

Discrete Fourier transform methods assume a repetitive function of time convolved with a rectangular window which covers the interval of the time domain sample. The results of this assumption are both beneficial and detrimental. The benefit is that a non-recurrent wave, such as the response to impact, may be objectively analyzed. The detriment is that an artifact-leakage⁽²⁾ may occur if the time domain constituents are not harmonically related to the sample window.

A method of minimizing this "leakage" is to shape the time domain information with a cosine or Hanning window, as illustrated in Figure 6. The Hanning weighting,

$$A = 0.5(1 - 2\pi t/T) \text{ for } t = 0 \text{ to } T,$$

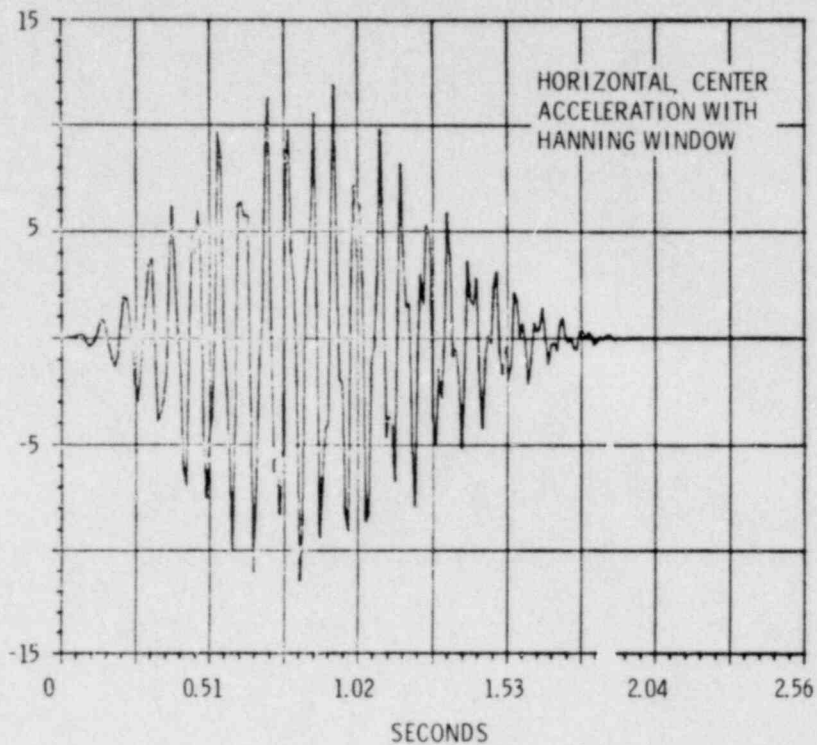
while reducing the leakage, preserves the amplitude information in the frequency domain. The amplitude of frequency domain parameters, when shaped with the Hanning window, is scaled by 0.5 if the information is uniform in the sample interval.

The example shown in Figure 6 illustrates that the spectral information for both the weighted and original data are similar, while their corresponding time domain representations are quite different.

These simple exercises in data analysis illustrate some of the fundamental techniques proposed for the analysis of the experimental data and, ultimately, model verification. Graphical data presentation may be em-

D2XRC

1E 3



MAGNITUDE OF FFT D2XRC

1E 3

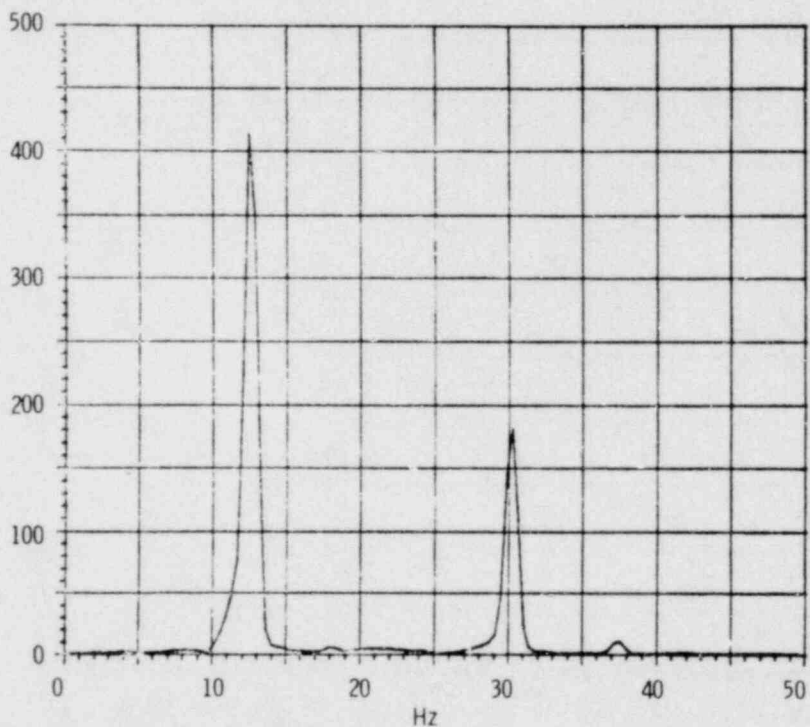
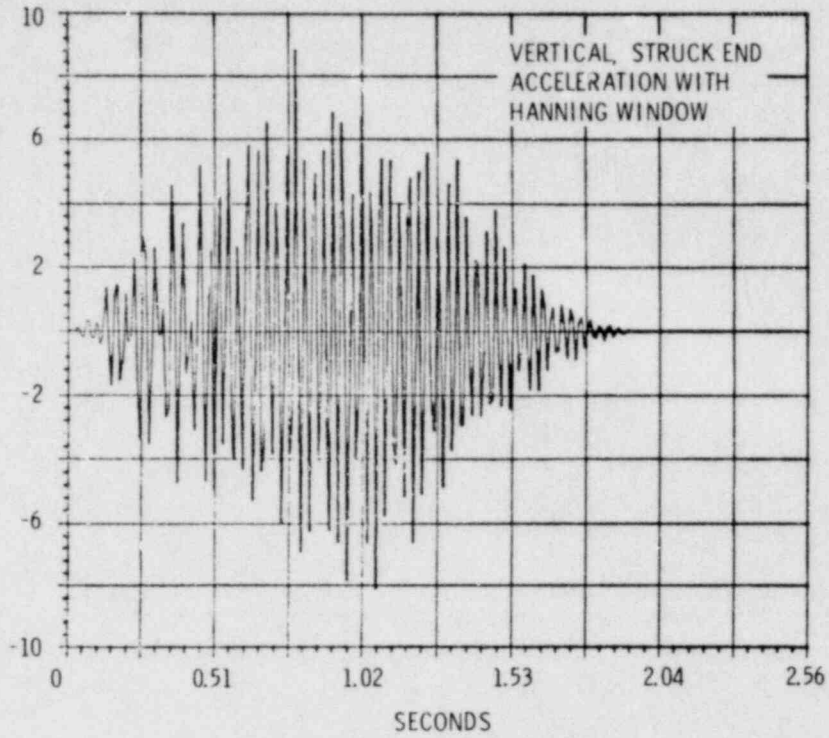


FIGURE 6a. Hanning Window Effect on Power Spectra When Applied to Time Domain Data.

1E3 - D2YR56



MAGNITUDE OF FFT D2YR56

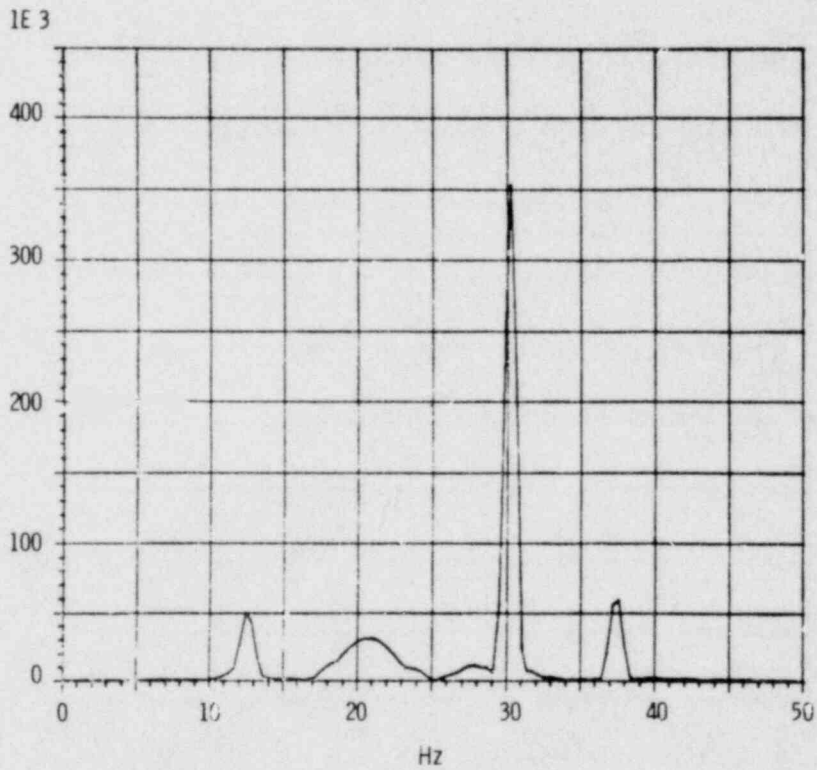


FIGURE 6b. Hanning Window Effect on Power Spectra When Applied to Time Domain Data.

ployed to assist in comparing the analytical model with the photographic data. An example of this technique is illustrated in Figure 7. This is a pseudo-isometric display of acceleration and displacement of the three points on the rail car as they vary with time.

3. Validate Model

Because of the restrictions of the proposed data analysis techniques, it would be pure chance that data generated analytically and that obtained experimentally would be comparable in their time domain form. The technique that will be initially employed to reduce the experimental data is as follows:

- Digitize all acceleration information with attention given to a consistent time scale with respect to impact.
- Assure that the time sample, t , for each digital representation conforms to

$$t < \frac{1}{2f_h}$$

where f_h is the highest frequency of interest in the measurement.

- Scale the time domain information with Hanning window.
- Repeat the operation for data generated from the analytical model.

Once the power spectra are in the same form, the model's parameters may be adjusted to force agreement.

During subsequent data analysis, techniques such as transfer function computation and filtering may be employed to validate the model.

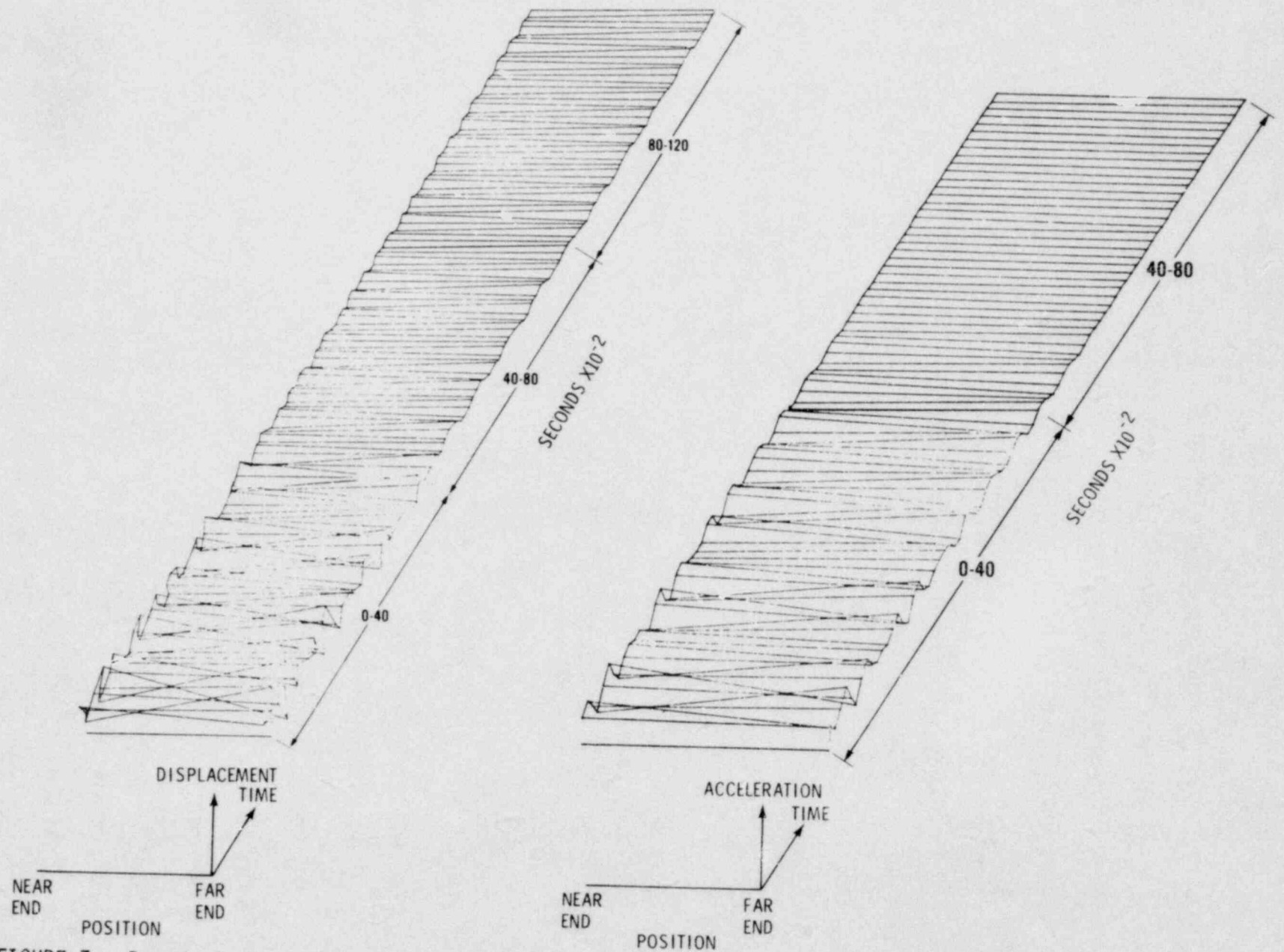


FIGURE 7. Pseudo-Isometric Illustrations of Car Acceleration and Displacement as It Varies with Time.

4. Collect Parameter Data

The collection of parameter data has been deferred until the next reporting period. During the next quarter, increased effort will be devoted to obtaining information on rail car suspension subsystem and coupler subsystem components.

5. Parametric and Sensitivity Analysis

This task is not scheduled to begin until December 1, 1978 (see Figure 1).

6. Interim Report

This report is not scheduled for preparation until August 1, 1978 (see Figure 1).

7. Final Report

This report is not scheduled for preparation until August 1, 1979 (see Figure 1).

REFERENCES

1. S. R. Fields, Dynamic Analysis to Establish Normal Shock and Vibration Environments Experienced by Radioactive Materials Shipping Packages, HEDL-TME 78-19 (NUREG/CR-0071), Hanford Engineering Development Laboratory, May 1978.
2. R. W. Ramirez, The FFT: Fundamentals and Concepts, Tektronix, Inc., Beaverton, OR, 1975.

DISTRIBUTION

DOE Richland Operations Office (4)
P. O. Box 550
Richland, WA 99352

Manager
Chief Patent Attorney
J. D. White

DOE FFTF Project Office (2)
P. O. Box 550
Richland, WA 99352

Director

DOE Chicago Patent Group
9500 S. East Avenue
Argonne, IL 60439

A. A. Churm

DOE Environmental Control Technology Division
Washington, DC 20545

J. Counts

Hanford Engineering Development Laboratory (35)
P.O. Box 1970
Richland, WA 99352

S. R. Fields

Pacific Northwest Laboratory
P.O. Box 999
Richland, WA 99352

L. D. Williams

E. I. DuPont de Nemours and Company
P.O. Box A
Aiken, SC 29801

S. F. Petry

DISTRIBUTION (cont'd)

Los Alamos Scientific Laboratory
P.O. Box 1663
Los Alamos, NM 87545

T. D. Butler

Sandia Laboratories
Albuquerque, NM 87115

C. F. Magnuson

NRC FORM 335 (7-77)		U.S. NUCLEAR REGULATORY COMMISSION BIBLIOGRAPHIC DATA SHEET		1. REPORT NUMBER (Assigned by DDC) NUREG/CR-0448	
4. TITLE AND SUBTITLE (Add Volume No., if appropriate) Dynamics Analysis to Establish Normal Shock and Vibration of Radioactive Material Shipping Package				2. (Leave blank)	
7. AUTHOR(S) S. R. Fields, S. J. Mech				5. DATE REPORT COMPLETED MONTH July YEAR 1978	
9. PERFORMING ORGANIZATION NAME AND MAILING ADDRESS (Include Zip Code) Hanford Engineering Development Laboratory P. O. Box 1920 Richland, WA 79352				DATE REPORT ISSUED MONTH December YEAR 1978	
12. SPONSORING ORGANIZATION NAME AND MAILING ADDRESS (Include Zip Code) Office of Nuclear Regulatory Research U. S. Nuclear Regulatory Commission Washington, D. C. 20555				6. (Leave blank)	
13. TYPE OF REPORT Quarterly				8. (Leave blank)	
15. SUPPLEMENTARY NOTES				10. PROJECT/TASK/WORK UNIT NO.	
16. ABSTRACT (200 words or less) <p>This report presents work performed at the Hanford Engineering Development Laboratory operated by Westinghouse Hanford Company, a subsidiary of Westinghouse Electric Corporation, for the Nuclear Regulatory Commission, under Department of Energy Contract No. EY-76-C-14-2170. It describes technical progress made during the reporting period by Westinghouse Hanford Company and supporting contractors.</p>				11. CONTRACT NO. NRC-60-78-354	
17. KEY WORDS AND DOCUMENT ANALYSIS				PERIOD COVERED (Inclusive dates) April 1, 1978-June 30, 1978	
17b. IDENTIFIERS/OPEN-ENDED TERMS				14. (Leave blank)	
18. AVAILABILITY STATEMENT Unlimited		19. SECURITY CLASS (This report)		21. NO. OF PAGES	
20. SECURITY CLASS (This page)		22. PRICE \$			